

1 **Nonlinear analysis of the occurrence of hurricanes in the Gulf of** 2 **Mexico and the Caribbean Sea**

3 Berenice Rojo-Garibaldi¹, David Alberto Salas-de-León², María Adela Monreal-Gómez², Norma
4 Leticia Sánchez-Santillán³, and David Salas-Monreal⁴

5 ¹Posgrado en Ciencias del Mar y Limnología, Universidad Nacional Autónoma de México, Av.
6 Universidad 3000, Col. Copilco, Del. Coyoacán, Cd. Mx. 04510, México.

7 ²Instituto de Ciencias del Mar y Limnología, Universidad Nacional Autónoma de México, Av.
8 Universidad 3000, Col. Copilco, Del. Coyoacán, Cd. Mx. 04510, México.

9 ³Departamento El Hombre y su Ambiente, Universidad Autónoma Metropolitana, Calz. del Hueso
10 1100, Del. Coyoacán, Villa Quietud, Cd.Mx. 04960, México.

11 ⁴Instituto de Ciencias Marinas y Pesquerías, Universidad Veracruzana, Hidalgo No. 617, Col. Río
12 Jamapa, C.P. 94290 Boca del Río, Veracruz, México.

13 Correspondence to D. A. Salas-de-León (dsalas@unam.mx)

14 **Abstract.** Hurricanes are complex systems that carry large amounts of energy. Their impact often
15 produces natural disasters involving the loss of human lives and materials, such as infrastructure,
16 valued in billions of US dollars. However, not everything about hurricanes is negative, as
17 hurricanes are the main source of rainwater for the regions where they develop. This study shows
18 a nonlinear analysis of the time series obtained from 1749 to 2012 of the occurrence of hurricanes
19 in the Gulf of Mexico and the Caribbean Sea. The construction of the hurricane time series was
20 carried out based on the hurricane database of the North Atlantic-basin Hurricane Database
21 (HURDAT) and the published historical information. The hurricane time series provides a unique
22 historical record on information about ocean-atmosphere interactions. The Lyapunov exponent
23 indicated that the system presented chaotic dynamics, and the spectral analysis and nonlinear
24 analyses of the time series of the hurricanes showed chaotic edge behavior. One possible
25 explanation for this edge is the individual chaotic behavior of hurricanes, either by category or
26 individually, regardless of their category and their behavior on a regular basis.

27 **Introduction**

28 Hurricanes have been studied since ancient times, and their activity is related to disasters and loss
29 of life. In recent years, there has been considerable progress in predicting their trajectory and
30 intensity once tracking them has begun, as well as their number and intensity from one year to the
31 next. However, their long-term and very short-term prediction remains a challenge (Halsey and
32 Jensen, 2004), and the damage to both materials and lives remains considerable. Therefore, it is
33 important to make a greater effort in the study of hurricanes to reduce the damage they cause. The
34 periodic behavior of hurricanes and their relationships with other natural phenomena have usually
35 been performed with linear-type analyzes which have provided valuable information. However,
36 we decided to make a different contribution by carrying out a nonlinear analysis of a time series of
37 hurricanes that occurred in the Gulf of Mexico and the Caribbean Sea, since the dynamics of the
38 system is controlled by a set of variables of low dimensionality (Gratrix and Elgin, 2004;
39 Broomhead and King, 1986).

40 One of the core parts of this work was the elaborate time series that was built, especially for the
41 oldest part of the registry, in which it was possible to have a substantial and robust collection. This
42 gave our time series a number of data with which it was possible to perform this analysis;
43 otherwise, it would have been impossible to study this natural phenomenon with a nonlinear
44 analysis.

45 Different methods have been used in the analysis of non-linear, non-stationary and non-Gaussian
46 processes, including artificial neural networks (ASCE Task Committee, 2000, Maier and Dandy,
47 2000, Maier et al., 2010, Taormina et al. 2015). Chen et al. (2015) use a hybrid neural network
48 model to forecast the flow of the Altamaha River in Georgia; Gholami et al. (2015) simulate
49 groundwater levels using dendrochronology and an artificial neural network model for the
50 southern Caspian coast in Iran. On the other hand, theories of deterministic chaos and fractal
51 structure have already been applied to atmospheric boundary data (Tsonis and Elsner, 1988; Zeng
52 et al., 1992), e.g., to the pulse of severe rain time series (Sharifi et al., 1990; Zeng et al., 1992) and
53 to the tropical cyclone trajectory (Fraedrich and Leslie, 1989; Fraedrich et al., 1990). Natural
54 phenomena occur in nature within different contexts; however, they often exhibit common
55 characteristics, or they may be understood using similar concepts. Deterministic chaos and fractal
56 structure in dissipative dynamical systems are among the most important nonlinear paradigms

57 (Zeng et al., 1992). For a detailed analysis of deterministic chaos, the Lyapunov exponent is
58 utilized as a key point and several methods have been developed to calculate it. It is possible to
59 define different Lyapunov exponents for a dynamic system. The maximal Lyapunov exponent can
60 be determined without the explicit construction of a time-series model. A reliable characterization
61 requires that the independence of the embedded parameters and the exponential law for the growth
62 of distances can be explicitly tested (Rigney et al., 1993; Rosenstein et al., 1993). This exponent
63 provides a qualitative characterization of the dynamic behavior and the predictability measurement
64 (Atari et al., 2003). The algorithms usually employed to obtain the Lyapunov exponent are those
65 proposed by Wolf (1986), Eckmann and Ruelle (1992), Kantz (1994) and Rosenstein et al. (1993).
66 The methods of Wolf (1986) and Eckmann and Ruelle (1992) assume that the data source is
67 indeed a deterministic dynamic system and that irregular fluctuations in time-series data are due to
68 deterministic chaos. A blind application of this algorithm to an arbitrary set of data will always
69 produce numbers, i.e., these methods do not provide a strong test of whether the calculated
70 numbers can actually be interpreted as Lyapunov exponents of a deterministic system (Kantz et
71 al., 2013). The Rosenstein et al. (1993) method follows directly from the definition of the
72 Lyapunov maximal exponent and is accurate because it takes advantage of all available data. The
73 algorithm is fast, easy to implement, and robust to changes in the following quantities: embedded
74 dimensions, data-set size, delay reconstruction, and noise level. The Kantz (1994) algorithm is
75 similar to that of Rosenstein et al. (1993).

76 We constructed a database of occurrences of hurricanes in the Gulf of Mexico and the Caribbean
77 Sea to perform a nonlinear analysis of the time series, the results of which can help in the
78 construction of hurricane occurrence models, and this in turn will help to reinforce the measures of
79 prevention for this type of hydrometeorological phenomenon.

80

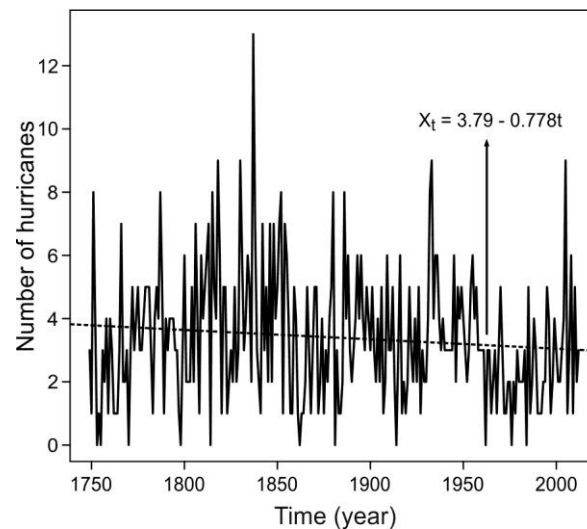
81 **2 Materials and methods**

82 **2.1 Data set description**

83 A detailed analysis of the historical reports, provided by the ships that were used, was carried out
84 in order to obtain the annual time series of the occurrence of hurricanes, from category one to five
85 on the Saffir-Simpson scale, in the study region from 1749-2012. The time series was composed

86 by the historical ship track of all vessels sailing close to registered hurricanes, the aerial
87 reconnaissance data for hurricanes since 1944 and the hurricanes reported by Fernández-Partagas
88 and Díaz (1995a, 1995b; 1996a; 1996b; 1996c; 1997; 1999). All this information in addition to the
89 database of the HURDAT re-analysis project (HURDAT is the official record of the United States
90 for tropical storms and hurricanes occurring in the Atlantic Ocean, Gulf of Mexico and Caribbean
91 Sea) was used in a comparative way in order to build our time series, which is so far the longest
92 time series of hurricanes for the Gulf of Mexico and the Caribbean Sea. This makes our series
93 ideal for performing a nonlinear analysis, which would be impossible with the records that are
94 available in other regions. All this information was used to build the hurricane time series (Fig. 1).

95



96

97 Figure 1. Hurricanes in the years 1749-2012. The line shows their linear trend (after Rojo-
98 Garibaldi et al., 2016).

99

100 Historical hurricanes were included only if they were reported in two or more databases and met
101 both of the following criteria: the reported hurricanes that touched land and those that remained in
102 the ocean; on the other hand, the followed hurricanes were studied considering their average
103 duration and their maximum time (9 and 19 days, respectively). This was done in order to avoid
104 counting more than one specific hurricane reported in different places within a short period time;
105 to do this, we followed the proposed method by Rojo-Garibaldi et al. (2016).

106

107 **2.2 Data reduction and procedures**

108 Before performing the nonlinear analysis of the time series, we removed the trend; thus, the series
109 was prepared according to what is required for this type of analysis. To know the properties of the
110 system requires more than estimating the dimensions of the attractor (Jensen et al., 1985); so, three
111 methods were applied in this study: 1) The Hurst exponent is a measure of the independence of the
112 time series as an element to distinguish a fractal series. It is basically a statistical method that
113 provides the number of occurrences of rare events and is usually called re-scaling (RS) rank
114 analysis (Gutiérrez, 2008); in addition, according to Miramontes and Rohani (1998), the Hurst
115 exponent provides another approximation that can be used to characterize the color of noise, and
116 therefore, it could be applied to any time series. The RS helps to find the Hurst exponent, which
117 provides the numerical value that makes it possible to determine the autocorrelation in a data
118 series. 2) The Lyapunov exponent is invariant under soft transformations, because it describes
119 long-term behavior, providing an objective characterization of the corresponding dynamics (Kantz
120 and Schreiber, 2004). The presence of chaos in dynamic systems can be solved by this exponent,
121 since it quantifies the exponential convergence or divergence of initially close trajectories in the
122 state space and estimates the amount of chaos in a system (Rosenstein et al., 1993; Haken, 1981;
123 Wolf, 1986). The Lyapunov exponent (λ) can take one of the following four values: $\lambda < 0$
124 corresponds to a stable fixed point, $\lambda = 0$ is for a stable limit cycle, $0 < \lambda < \infty$ indicates chaos and
125 $\lambda = \infty$ is a Brownian process, which agrees with the fact that the entropy of a stochastic process is
126 infinite (Kantz and Schreiber, 2004). 3) The iterated function analysis (IFS) is an easier and
127 simpler way to visualize the fine structure of the time series because it can reveal correlations in
128 the data and help to characterize its color, referring to color to the type of noise (Miramontes et al.,
129 2001). Together with the Lyapunov exponent, the phase diagrams, the False Close Neighbors
130 method, the Space-Time Separation plot, the Correlation Integral plot, and the Correlation
131 Dimension were taken into account, the latter two to identify whether the system attractor was a
132 fractal type. It is important to compute the Lyapunov exponent, so we used the algorithms
133 proposed by Kantz (1994) and Rosenstein et al. (1993) to calculate it.

134

135 **3 Results and discussions**

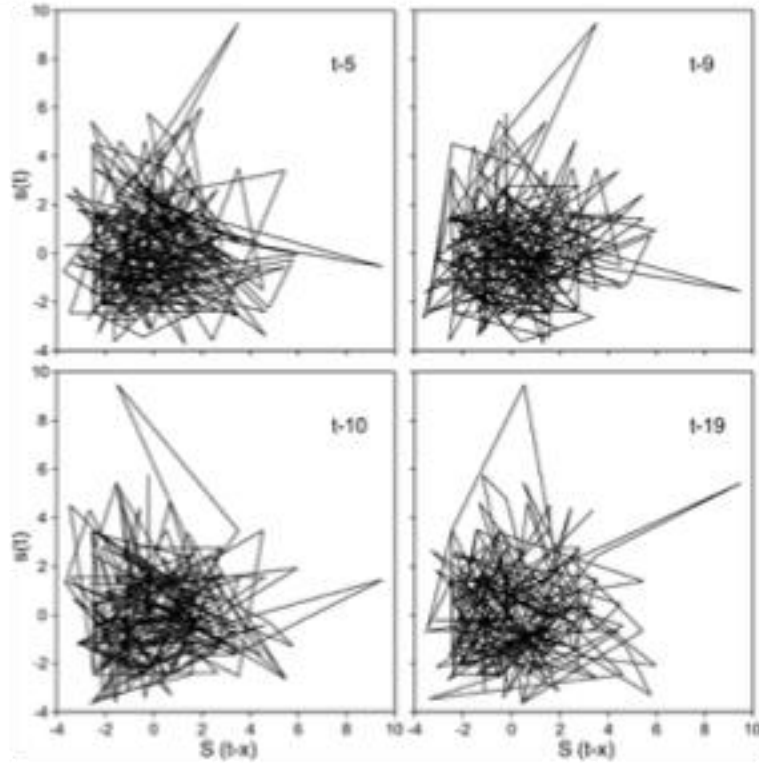
136 Figure 1 shows the evolution of the number of hurricanes from 1749 to 2012 and the linear trend.
137 To have a qualitative idea of the behavior of the number of hurricanes that occurred in the Gulf of
138 Mexico and the Caribbean Sea from 1749 to 2012, a phase diagram was performed using the
139 “delay method” (Fig. 2). This was also used to elucidate the time lag for an optimal embedding in
140 the dataset. The optimal time lag (τ) obtained visually from Fig. 2 was equal to 9, since it was the
141 time in which the curves of the system were better divided. We must not forget that this was only
142 a visual inspection, and the delay time will be obtained quantitatively through other methods. In
143 our case, the hurricane dynamics were not distinguished through the phase diagram; however,
144 since any hurricane trajectory starts at a close point location on the attractor dataset that diverges
145 exponentially, the phase diagram is a primary evidence of a chaotic motion according to
146 Thompson and Stewart (1986).

147 The most robust method to identify chaos within the system is the Lyapunov exponent. Prior to
148 obtaining the exponent, it was necessary to calculate the time lag and the embedding dimension,
149 and for the latter, the window of Theiler was used. The time lag was obtained with three different
150 methods: 1) the method of constructing delays, which is observed visually in Figure 2; 2) the
151 method of mutual information, which yields a more reliable result since it takes into account
152 nonlinear dynamic correlations; here, the delay time was obtained by taking the first minimum of
153 the function; in this case $\tau = 9$; and 3) the autocorrelation function method, which is based solely
154 on linear statistics (Fig. 3).

155 There are two ways to obtain the time lag from the autocorrelation function: 1) the first zero of the
156 function, and 2) the moment in which the autocorrelation function decays as $1/e$ (Kantz and
157 Schreiber, 2004). We used the criterion of the first zero because the Hurst exponent ($H = 0.032$)
158 indicated that it was a short memory process; therefore, the criterion of the first zero is the optimal
159 method in this type of case. By this method, the value that was obtained was $\tau = 10$. The value of
160 this parameter is very important, since if it turns out to be very small, then each coordinate is
161 almost the same and the reconstructed trajectories look like a line (the phenomenon is known as
162 redundancy). On the other hand, if the delay time is quite large, then due to the sensitivity of the
163 chaotic movement, the coordinates appear to be independent and the reconstructed phase space

164 looks random or complex (a phenomenon known as irrelevance) (Bradley and Kantz, 2015).

165



166 Figure 2. Phase diagrams corresponding to the time series of hurricanes that occurred between the
167 years 1749 and 2012 in the Gulf of Mexico and the Caribbean Sea. The x - axis in the four plots
168 indicates the time lag (τ).
169

170

171 The Hurst exponent helps us to identify the criteria to find a time lag, and it also describes the
172 system behavior (Quintero and Delgado, 2011). This could indicate that the system does not have
173 chaotic behavior; however, the remaining methods have indicated the opposite, and as mentioned
174 previously, the Lyapunov exponent is considered the most appropriate method for this type of
175 dataset. Therefore, different methods will provide different results, but the time series will indicate
176 the best method and the result we should use.

177 It was possible to observe the difference in the time lag obtained through the autocorrelation

178 function and the mutual information; however, it is necessary to use only one result. Through the
 179 space-time separation graphic and the False Close Neighbors method, we obtained embedding
 180 dimensions of $m = 4$ for a $\tau = 9$ and $m = 5$ for $\tau = 10$, and the Theiler window with a value of $W =$
 181 16 for $\tau = 9$ and $W = 18$ for $\tau = 10$ (Fig. 4). The choice of this window is very important so as not
 182 to obtain subsequent spurious dimensions in the attractor. According to Bradley and Kantz (2015),
 183 the Theiler window ensures that the time spacing between the potential pairs of points is large
 184 enough to represent a distributed sample identically and independently.

185 The idea of the False Close Neighbors algorithm is that at each point in the time series, \bar{S}_t and its
 186 neighbor \bar{S}_j should be searched in a m -dimensional space. Thus, the distance $\|S_t - S_j\|$ is
 187 calculated iterating both points, given by:

188

$$189 \quad R_i = \frac{S_{i+1} - S_{j+1}}{\|\bar{S}_i - \bar{S}_j\|} \quad (1)$$

190

191 If R_i is greater than the threshold given by R_t , then S_j has false close neighbors. According to
 192 Kennel et al. (1992), a value of $R_t = 10$ has proven to be a good choice for most of the data set, but
 193 a formal mathematical proof for this conclusion is not known; therefore, if this value does not give
 194 convincing results, it is advisable to repeat the calculations for several R_t (Perc, 2006). In our case,
 195 this value gave relevant results. It may have some False Close Neighbors even when working with
 196 the correct embedding dimension. The result of this analysis may depend on the time lag (Kantz
 197 and Schreiber, 2004). In the same way as the delay time, the value of the embedment dimension is
 198 crucial not only for the reconstruction of the phase space but also to obtain the Lyapunov
 199 exponent. Choosing a large value of m for chaotic data will add redundancy and will affect the
 200 development of many algorithms such as the Lyapunov exponent (Kantz and Schreiber, 2004).

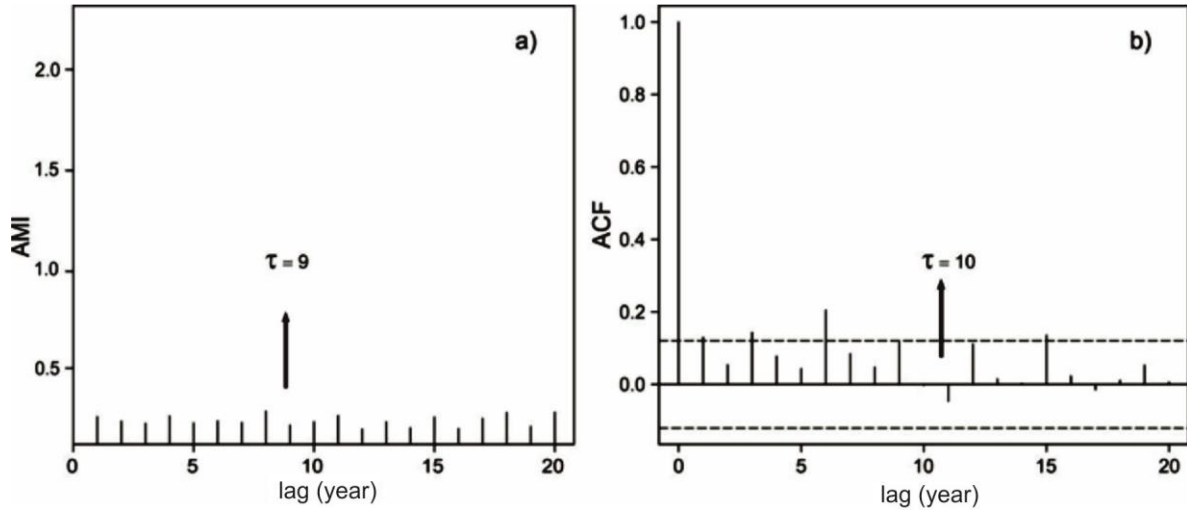
201 The Lyapunov (λ) exponents were obtained using the Kantz and Rosenstein methods and took the
 202 time lag, the embedding dimension and the Theiler window as the main values; nevertheless, an
 203 election of the neighborhood radius for the exploration of trajectories was also made, as well as
 204 the points of reference and the neighbors near these points. The modification of these parameters

205 is important to corroborate the invariant characteristic of the Lyapunov exponent. The Kantz
206 (1994) method using a value of $m = 4$ and $\tau = 9$ gave us an exponent of $\lambda = 0.483$, while for $m = 5$
207 and $\tau = 10$ the exponent was $\lambda = 0.483$. Since λ is a positive value, it was inferred that our system
208 is chaotic. In addition, the value of λ obtained for both imbibing dimensions was the same,
209 suggesting that our result is accurate. Using the Rosenstein et al. (1993) method, the value
210 obtained for $m = 4$ and $\tau = 9$ was $\lambda = 0.1056$, and for $m = 5$ and $\tau = 10$, the exponent was $\lambda =$
211 0.112 (Fig. 5).

212 There was a difference between placing the attractor in an embedding dimension of $m = 4$ and one
213 of $m = 5$; a better unfolding of the attractor in the embedding dimension was observed in $m = 4$
214 and $\tau = 9$. This value of τ was obtained with the mutual information method, which, according to
215 Fraser and Swinney (1986) and Krakovská et al. (2015), provides a better criterion for the choice
216 of delay time than the value obtained by the autocorrelation function.

217 It was possible to obtain the Correlation Dimension D_2 (Fig. 6) and the Correlation Integral (Fig.
218 6) using the embedding dimension, the delay time and the Theiler window, following the method
219 of Grassberger and Procaccia (1983a, 1983b). This was done in order to obtain the possible
220 dimensions of the attractor. It should be noted that there is a whole family of fractal dimensions,
221 which are usually known as Renyi dimensions, but these are based on the direct application of box
222 counting methods, which demands significant memory and processing and whose results can be
223 very sensitive to the length of the data (Bradley and Kantz, 2015). That is why we use the
224 Dimension and Integral Correlation, since according to Bradley and Kantz (2015) it is a more
225 efficient and robust estimator.

226



227
 228 Figure 3. The left panel shows the mutual information method; the x - axis indicates the time lag
 229 against the mutual information index (AMI) and the arrow indicates the first, most pronounced
 230 minimum with a value of $\tau = 9$. The right panel shows the autocorrelation function, the x - axis
 231 indicates the time lag versus the value of the autocorrelation function, and the arrow denotes
 232 where the first zero of the function $\tau = 10$ was obtained.

233

234 The right panel on Fig. 7 shows the slope trend of the majority of the slopes of the Correlation
 235 Integral (ε). In the range of $1 < \varepsilon < 10$, we are required to have straight lines as an indicator of the
 236 self-similar geometry. The value obtained here corresponds to $D_2 = 2.20$ which is the
 237 aforementioned slope value. Another method to see the attractor dimension is the Kaplan-Yorke
 238 Dimension (D_{ky}), which is associated with the spectrum of Lyapunov exponents and is given by:

239

$$240 \quad D_{KY} = k + \sum_{i=1}^k \frac{\lambda_i}{|\lambda_{k+1}|} \quad (2)$$

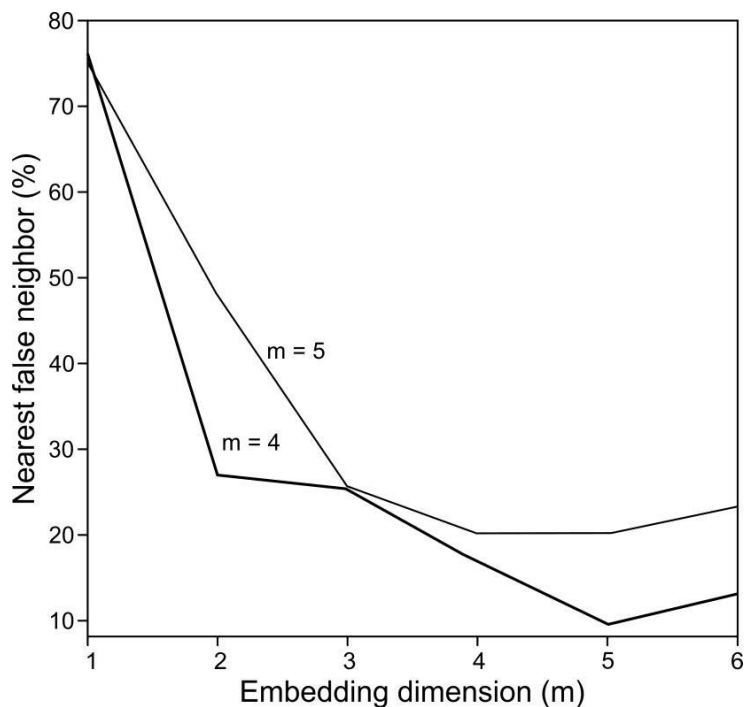
241

242 where k is the maximal integer, such that the sum of the k major exponents is not negative. The
 243 fractal dimension with this method yielded a value of $D_{ky} = 2.26$, which is similar to the one
 244 obtained previously.

245 Even when all the requirements necessary to apply the nonlinear analysis to our time series are

246 present, one final requirement must be fulfilled to know whether we can obtain a dimension and
247 whether the complete spectrum of Lyapunov exponents (another method to visualize chaos) still
248 needs to be employed.

249



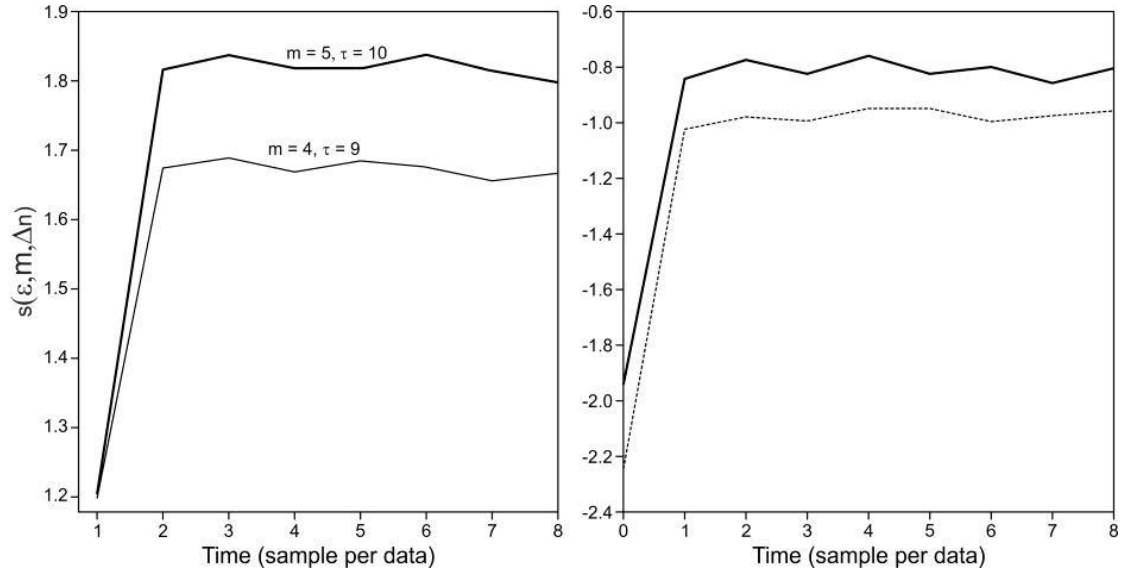
250

251

252 Figure 4. False Close Neighbors with a time lag of 10, where the embedding dimension of 5 has a
253 9.4% and the embedding dimension of 4 has a 16.66% False Close Neighbors (lower line). False
254 Close Neighbors with a time lag of 9, where the embedding dimension of 5 has a 20.15% and the
255 embedding dimension of 4 has a 20.12% False Close Neighbors (upper line). The values in each
256 line indicate the optimal dimension for each lag.

257

258 Eckmann and Ruelle (1992) discuss the size of the dataset required to estimate Lyapunov
259 dimensions and exponents. When these dimensions and exponents measure the divergence rate
260 with near-initial conditions, they require a number of neighbors for a given reference point. These
261 neighbors may be within a sphere of radius r and of a given diameter (d) of the reconstructed
262 attractor.



264

265 Figure 5. Left panel: Lyapunov exponent with $m = 4$, $\tau = 9$ and $m = 5$, $\tau = 10$, with the Kantz
 266 method. Right panel: Lyapunov exponent with the same values with the Rosenstein method.

267

268 In this way we have the requirement for the Eckmann and Ruelle (1992) condition to obtain the
 269 Lyapunov exponents as:

270

$$271 \quad \log N > D \log \left(\frac{1}{\rho} \right) \quad (3)$$

272

273 where D is the dimension of the attractor, N is the number of data points and $\frac{r}{d} = \rho$. For $\rho = 0.1$ in
 274 equation (3), N may be chosen such that:

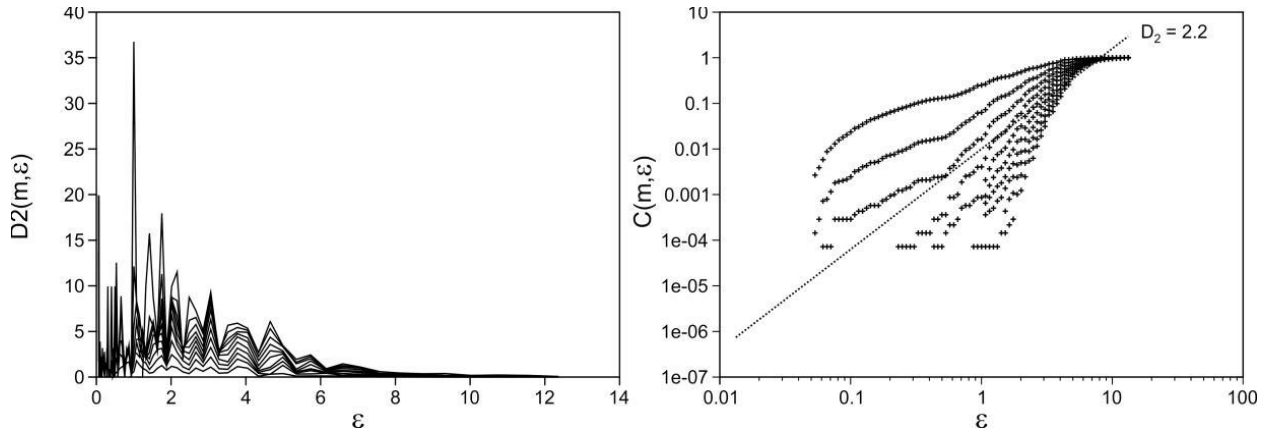
275

$$276 \quad N > 10^D \quad (4)$$

277

278 Our time series met this requirement; therefore, it supports our previous results.

279



280
281

282 Figure 6. The correlation dimension D_2 corresponding to the occurrence of hurricanes in the years
283 1749-2012 in the Gulf of Mexico and the Caribbean Sea. Left-panel: curves for different
284 dimensions of the attractor (y - axis). Right panel: same information for the D_2 with a logarithmic
285 scale on the x - axis.

286

287 The attractor dimension was mainly obtained because this value tells us the number of parameters
288 or degrees of freedom necessary to control or understand the temporal evolution of our system in
289 the phase space and helps us to know how chaotic our system is. Using the previous methods, a
290 final fractal dimension of $D_2 = 2.2$ was obtained. Following the embedding laws, it must be that m
291 $> D_2$ (Sauer and Yorke, 1993; Kantz and Schreiber, 2004; Bradley and Kantz, 2015). The criterion
292 of Ruelle (1990) was used to corroborate that the obtained dimension of the attractor is reliable,
293 where it must be that $N = 10^{\frac{D_2}{2}}$; once the data fulfill this requirement, we can say that the
294 dimension of the attractor is reliable. Finally, the results indicated that at least three parameters are
295 needed to characterize our system, since the 2.2 dimension indicates that the attractor dimension
296 falls between 2 and 3.

297 The spectrum of the Lyapunov exponent gives 0.09983, -0.07443, -0.23387 and -0.73958;
298 therefore, the total sum was $\lambda_i = -0.9480$, and according to the previous theory, it is enough have

299 at least one positive exponent in the spectrum of our system in order to have chaotic behavior.
300 Finally, the total sum of the spectrum of Lyapunov exponents was negative, indicating that there is
301 a stable attractor, as mentioned previously. However, since the stable attractor was not easily
302 distinguished, we used a final method in order to confirm if our system presented some chaotic
303 dynamic behavior. This method comprised the Iterated Functions System test (IFS) (Fig. 7).

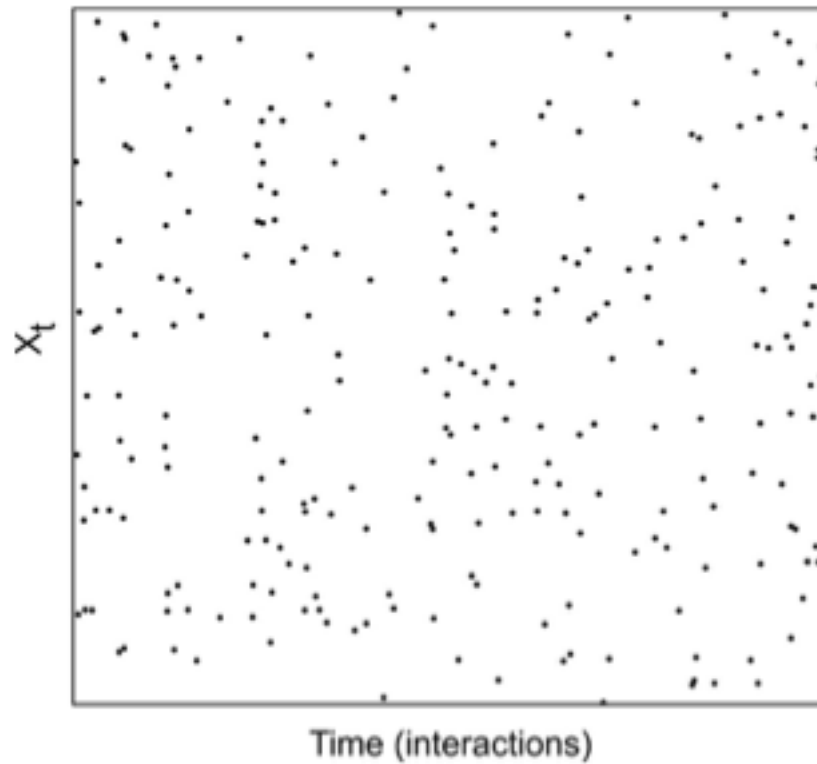
304 Using Fig. 7, it can be observed that the points representing our system occupy the entire space;
305 according to the IFS test, there are two possible explanations: 1) The distribution belongs to a
306 white noise signal and in systems without experimental noise, the point distribution gives a single
307 curve (Jensen et al., 1985). However, the previous Hurst exponent obtained was not equal to zero;
308 thus, the white noise was also discarded with the autocorrelation function. 2) The system is chaotic
309 of high dimensionality. So far, our results have converged on the occurrence of hurricanes in the
310 Gulf of Mexico and the Caribbean Sea being a chaotic system, so it is feasible to adopt the second
311 explanation. On the other hand, our Lyapunov exponent figure was not flat and it did not seem to
312 flatten as the dimension of embedding increased, which, according to Rosenstein et al. (1993),
313 would mean that our system is not chaotic. Similarly, the Lyapunov exponent increased with the
314 decrease in the embedment dimension, which is, again, a characteristic of chaotic systems. It was
315 then also possible to obtain a dimension of the attractor and a positive Lyapunov exponent.

316 Our results were not easy to interpret because the series presented certain periodic characteristics
317 in an oscillatory fashion and chaotic behavior at the same time. According to Rojo-Garibaldi et al.
318 (2016), the series of hurricanes with the spectral analyzes carried out presented strong periodicities
319 that correspond to sunspots, which gives the system the periodic behavior mentioned above.
320 According to Zeng et al. (1990), the spectral power analysis is often used to distinguish a chaotic
321 or quasi-periodic behavior of periodic structures and to identify different periods embedded in a
322 chaotic signal. Although, as Schuster (1988) and Tsonis (1992) mention, the power spectrum is
323 not only characteristic of a process of deterministic chaos but also of a linear stochastic process. In
324 our case, this behavior was not observed in the spectra obtained, which allowed us to detect
325 periodic signals. The spectra give our system two types of behavior. First, there are periodic
326 behaviors associated with external forcing, such as the sunspot cycle, giving the system sufficient
327 order to develop; on the other hand, external forcing presents a chaotic behavior, which gives the
328 system a certain disorder to be able to adapt to new changes and evolve. The IFS test showed that

329 the occurrence of hurricanes in the Gulf of Mexico and the Caribbean Sea is chaotic with high
330 dimensionality. Fraedrich and Leslie (1989) analyzed the trajectories of hurricanes in the region of
331 Australia and calculated the dimensionality of this process, obtaining a result of between 6 and 8,
332 i.e., a chaotic process of high dimensionality, which is similar to what we find with the IFS
333 method. On the other hand, Halsey and Jensen (2004) postulate that hurricanes contain a large
334 number of dimensions in phase space.

335 One possible explanation is localized within a boundary where chaos and order are separated; this
336 boundary is commonly known as the “edge of chaos” (Langton, 1990; Miramontes et al., 2001).
337 Miramontes et al. (2001) found this type of behavior in ants of the genus *Leptothorax*, when
338 studying them individually and in groups. In the former case, the behavior was periodic, while in
339 the latter, the behavior was chaotic. In our case, we believe that the chaotic behavior is due to the
340 individual behavior or the hurricane category, since the high dimensionality suggested by the IFS
341 test agrees with the high dimensionality reported by Fraedrich and Leslie (1989) obtained by
342 studying the trajectories of hurricanes, that is, by studying them individually, while the periodic
343 response is due to the behavior of hurricanes as a whole.

344



345
 346 Figure 7. The Iterated Functions System (IFS) test applied to the time series of the number of
 347 hurricanes that occurred in the Gulf of Mexico and the Caribbean Sea between the years 1749 and
 348 2012.

349

350 **4 Conclusions**

351 The results obtained with the nonlinear analysis suggested a chaotic behavior in our system,
 352 mainly based on the Lyapunov exponents and correlation dimension, among others. However, the
 353 Hurst exponent indicated that our system did not follow a chaotic behavior, and in order to be able
 354 to corroborate our results, we employed the IFS method, which led us to think that the hurricane
 355 time series in the Gulf of Mexico and the Caribbean Sea from 1749 to 2012 had a chaotic edge. It
 356 is important to emphasize that this study was prepared as an attempt to understand the behavior of
 357 the occurrence of hurricanes from a historical perspective, since this type of phenomenon is part of
 358 an ocean-atmosphere interaction that has been changing over time, hence the value of our

359 contribution. However, we are aware that from the time the study was conducted to the present
360 date there are new records, which will make it possible to carry out new studies applying new
361 methods.

362

363 *Author contributions.* All the authors contributed equally to this work.

364 *Competing interests.* The authors declare that they have no conflicts of interest.

365 *Acknowledgements.* This work was financially supported by the Instituto de Ciencias del Mar y
366 Limnología de la Universidad Nacional Autónoma de México, projects 144 and 145. BR-G is
367 grateful for the CONACYT Scholarship that supported her study at the Posgrado en Ciencias del
368 Mar y Limnología, Universidad Nacional Autónoma de México.

369

370 **References**

- 371 ASCE Task Committee on Application of Artificial Neural Networks in Hydrology: Application
372 of artificial neural networks in hydrology. I: Preliminary concepts. *J. Hydrol. Eng.* 5, 115–123,
373 2000.
- 374 Ataei, M., Khaki-Sedigh, A., Lohmann, B. and Lucas, C.: Determining embedding dimension
375 from output time series of dynamical systems-scalar and multiple output cases, in: *Proceedings of*
376 *the 2nd International Conference on System Identification and Control Problems*, Moscow, Russia,
377 p. 1004-13, 2003.
- 378 Bradley, E. and Kantz, H.: Nonlinear time-series analysis revisited, *Chaos*, 25, 097610-1-097610-
379 10, 2015.
- 380 Broomhead, D. S. and King, G. P.: Extracting qualitative dynamics from experimental data.
381 *Physica D: Nonlinear Phenomena*, 20(2-3), 217-236, 1986.
- 382 Bountis, T., Karakasidis, L., Papaioannou, G. and Pavlos, G.: Determinism and noise in surface
383 temperature time series. *Ann. Geophysicae*, 11, 947-959, 1993.
- 384 Chen, X.Y., Cahu, K-W., and Busari, A. O.: “A comparative study of population-based
385 optimization algorithms for downstream river flow forecasting by a hybrid neural network model,”
386 *Engineering Applications of Artificial Intelligence* 46 (A): 258-268, 2015.
- 387 Quintero, O. Y. and Delgado, J. R.: Estimación del exponente de Hurst y la dimensión fractal de
388 una superficie topográfica a través de la extracción de perfiles, *Geomática UD.GEO*, 5, 84-91, In
389 Spanish, 2011.
- 390 Eckmann, J. P. and Ruelle, D.: Fundamental limitations for estimating dimensions and Lyapunov
391 exponents in dynamical systems, *Physica D*, 56, 185-187, 1992.
- 392 Fernández-Partagás, J. J. and Díaz, H. F.: A reconstruction of historical tropical cyclone frequency
393 in the Atlantic from documentary and other historical sources. Part I, 1851- 1870, *Climate*

- 394 Diagnostics Center, Environmental Research Laboratories, NOAA, Boulder, CO., 1995a.
- 395 Fernández-Partagás, J. J. and Díaz, H. F.: A reconstruction of historical tropical cyclone frequency
396 in the Atlantic from documentary and other historical sources. Part II, 1871-1880, Climate
397 Diagnostics Center, Environmental Research Laboratories, NOAA, Boulder, CO., 1995b.
- 398 Fernández-Partagás, J. J. and Díaz, H. F.: Atlantic hurricanes in the second half of the nineteenth
399 century, *B. Am. Meteorol. Soc.*, 77, 2899-2906, 1996a.
- 400 Fernández-Partagás, J. J. and Díaz, H. F.: A reconstruction of historical tropical cyclone frequency
401 in the Atlantic from documentary and other historical sources. Part III, 1881-1890, Climate
402 Diagnostics Center, Environmental Research Laboratories, NOAA, Boulder, CO., 1996b.
- 403 Fernández-Partagás, J. J. and Díaz, H. F.: A reconstruction of historical tropical cyclone frequency
404 in the Atlantic from documentary and other historical sources. Part IV, 1891-1900, Climate
405 Diagnostics Center, Environmental Research Laboratories, NOAA, Boulder, CO., 1996c.
- 406 Fernández-Partagás, J. J. and Díaz, H. F.: A reconstruction of historical tropical cyclone frequency
407 in the Atlantic from documentary and other historical sources. Part V, 1901-1908, Climate
408 Diagnostics Center, Environmental 320 Research Laboratories, NOAA, Boulder, CO., 1997.
- 409 Fernández-Partagás, J. J. and Díaz, H. F.: A reconstruction of historical tropical cyclone frequency
410 in the Atlantic from documentary and other historical sources. Part VI, 1909-1910, Climate
411 Diagnostics Center, Environmental Research Laboratories, NOAA, Boulder, CO., 1999.
- 412 Fraedrich, K. and Leslie, L.: Estimates of cyclone track predictability. I: Tropical cyclones in the
413 Australian region? *Q.J.R. Meteorol. Soc.*, 115, 79-92, 1989.
- 414 Fraedrich, K., Grotjahn, R., and Leslie, L. M.: Estimates of cyclone track predictability. II: Fractal
415 analysis of mid-latitude cyclones, *Q. J. Roy. Meteor. Soc.*, 116, 317-335, 1990.
- 416 Gholami, V., Chau, K-W., Fadaie, F., Torkaman, J., and Ghaffari, A.: “Modeling of groundwater
417 level fluctuations using dendrochronology in alluvial aquifers”, *Journal of Hydrology* 529 (3):
418 1060-1069, 2015.

419 Gratrix, S. and Elgin, J. N.: Pointwise dimensions of the Lorenz attractor. *Physical Review*
420 *Letters*, 92(1), 014101, 2004.

421 Gutiérrez, H.: Estudio de geometría fractal en roca fracturada y series de tiempo, M. Sc. Thesis,
422 Universidad de Chile, Facultad de Ciencias Físicas y Matemáticas, Departamento de Ingeniería
423 Civil, Santiago de Chile, Chile, In Spanish, 2008.

424 Halsey, T. C. and Jensen, M. H.: Hurricanes and butterflies. *Nature*, 428(6979), 127-128, 2004.

425 Haken H.: Chaos and Order 5 in Nature. In: Haken H. (eds) *Chaos and Order in Nature*. Springer
426 *Series in Synergetics*, vol 11. Springer, Berlin, Heidelberg, 1981.

427 Hegger, R., Kantz H. and Schreiber, T.: Practical implementation of nonlinear time series
428 methods: The Tisean package, *Chaos*, 9, 413-435, 1999.

429 Jensen, M. H., Kadanoff, L. P., Libchaber, A., Procaccia, I. and Stavans, J.: Global universality at
430 the onset of chaos: results of a forced Rayleigh-Bénard experiment. *Physical Review Letters*,
431 55(25), 2798, 1985.

432 Kantz, H.: A robust method to estimate the maximal Lyapunov exponent of a time series, *Phys.*
433 *Lett. A*, 185, 77-87, 1994.

434 Kantz, H. and Schreiber, T.: *Nonlinear time series analysis*, Vol. 7, Cambridge University Press,
435 Cambridge, 2004.

436 Kantz, H., Radons G. and Yang H.: The problem of spurious Lyapunov exponents in time series
437 analysis and its solution by covariant Lyapunov vectors. *J. Phys. A: Math. Theor.*, 46, 254009.

438 Kennel, M. B., Brown, R. and Abarbanel, H. D. I.: Determining embedding dimension for phase-
439 space reconstruction using a geometrical construction, *Phys. Rev. A* 45, pp. 3403, 1992.

440 Krakovská, A., Mezeiová, K. and Budáková, H.: Use of False Nearest Neighbours for Selecting
441 Variables and Embedding Parameters of State Space Reconstruction, *Journal of Complex*
442 *Systems*, pp. 1-12, 2015.

- 443 Langton, C. G.: Computation at the edge of chaos: phase transitions and emergent computation,
444 *Physica D*, 42, 12-37, 1990.
- 445 Maier, H.R., Jain, A., Dandy, G.C., Sudheer, K.P.: Methods used for the development of neural
446 networks for the prediction of water resource variables in river systems: current status and future
447 directions. *Environ. Model. Softw.* 25, 891–909, 2010.
448 <http://dx.doi.org/10.1016/j.envsoft.2010.02.003>.
- 449 Maier, H.R., Dandy, G.C.: Neural networks for the prediction and forecasting of water resources
450 variables: a review of modelling issues and applications. *Environ. Model. Softw.* 15, 101–124,
451 2000. [http://dx.doi.org/10.1016/S1364-8152\(99\)00007-9](http://dx.doi.org/10.1016/S1364-8152(99)00007-9).
- 452 Miramontes, O., Sole, R. V. and Goodwin, B. C.: Neural networks as sources of chaotic motor
453 activity in ants and how complexity develops at the social scale, *Int. J. Bifurcat. Chaos*, 11, 1655-
454 1664, 2001.
- 455 Miramontes, O. and Rohani. P.: Intrinsically generated coloured noise in laboratory insect
456 populations, *R. Soc.*, 265, 785-792, 1998.
- 457 Perc, M.: Introducing nonlinear time series analysis in undergraduate courses, *FISIKA A*, 15, 2,
458 pp. 91-112, 2006.
- 459 Rigney, D. R., Goldberger, A. L., Ocasio, W., Ichimaru, Y., Moody, G. B., Mark, R.: Multi-
460 Channel Physiological Data: Description and Analysis, in Weigend, A. S., Gershenfeld, N. A.,
461 Eds: *Predicting the Future and Understanding the Past: A Comparison of Approaches*. Santa Fe
462 Institute Studies in the Science of Complexity, Proc. Vol. XV, Addison-Wesley, Reading, MA.,
463 1993.
- 464 Rojo-Garibaldi, B., Salas-de-León, D. A., Sánchez, N. L. and Monreal-Gómez, M. A.: Hurricanes
465 in the Gulf of Mexico and the Caribbean Sea and their relationship with sunspots, *J. Atmos. Sol.-*
466 *Terr. Phy.*, 148, 48-52, 2016.
- 467 Rosenstein, M. T., Collins, J. J. and De Luca, C. J.: A practical method for calculating largest
468 Lyapunov exponents from small data sets, *Physica D*, 65, 117-134, 1993.

- 469 Ruelle, R.: Deterministic chaos: The science and the fiction, Proc. R. Soc. London, A427, pp. 241-
470 248, 1990.
- 471 Sauer, T. and Yorke J. A.: How many delay coordinates do you need? Int. J. Bifurcat. Chaos, 3,
472 737-744, 1993.
- 473 Schuster, H.: Deterministic Chaos, 2nd ed. Physik-Verlag, Weinheim, Germany, 1988.
- 474 Sharifi, M., Georgakakos, K. and Rodriguez-Iturbe, I.: Evidence of deterministic chaos in the
475 pulse of storm rainfall, J. Atmos. Sci., 47, 888-893, 1990.
- 476 Taormina, R., Chau, K-W., and Sivakumar, B.: “Neural network river forecasting through
477 baseflow separation and binary-coded swarm optimization”, Journal of Hydrology 529 (3): 1788-
478 1797, 2015.
- 479 Thompson, J. and Stewart, H.: Nonlinear dynamics and chaos: geometrical methods for engineers
480 and scientists, John Wiley 30 & Sons Ltd, New York, 1986.
- 481 Tsonis, A.: Chaos: From Theory to Application, Plenum, New York, 1992.
- 482 Tsonis, A. and Elsner, J.: The weather attractor over very short timescales, Nature 333, 545-547,
483 1988.
- 484 Wolf, A.: Quantifying chaos with Lyapunov exponents, Princeton University Press, Princeton, NJ,
485 1986.
- 486 Zeng, X., Pielke, R. and Eykholt, R.: Estimating the fractal dimension and the predictability of the
487 atmosphere, J. Atmos. Sci., 49, 649-659, 1992.
- 488 Zeng, X., Pielke, R. A., Eykholt, R.: Chaos in daisyworld, *Tellus*, 42B, pp. 309-318, 1990.